Am J Cancer Res 2021;11(1):157-170
www.ajcr.us /ISSN:2156-6976/ajcr0120358

Original Article

RBM10 regulates human TERT gene splicing and inhibits pancreatic cancer progression

Wenjing Xiao[1,3*], Xin Chen[2*], Xia Li[4*], Kaiwen Deng[3], Huawei Liu[2], Jie Ma[3], Zhanhao Wang[2], Yonghe Hu[1,3], Jun Hou[3]

[1]*School of Materials Science and Engineering, Southwest Jiaotong University, Chengdu 611756, China;* [2]*Department of Laboratory Medicine, The Third People's Hospital of Chengdu/Affiliated Hospital of Southwest Jiaotong University, Chengdu 610015, China;* [3]*Department of Pharmacy, The General Hospital of Western Theater Command of PLA, Chengdu 610083, China;* [4]*Department of Ultrasound Diagnosis, Women and Children's Health Care Hospital of Linyi, Linyi 276000, China.* [*]*Equal contributors.*

Received August 14, 2020; Accepted October 14, 2020; Epub January 1, 2021; Published January 15, 2021

Abstract: Dysregulation of alternative splicing of hTERT gene to generate full-length Htert (hTERT-FL) that reactivate telomerase has been recognized as a major pathological alteration in pancreatic cancer (PrCa). Mechanism about the factors that regulate hTERT-FL splicing is lacking. Through bioinformatics approach, we focus on a candidate splicing factor RBM10, which leads to a switch in hTERT transcripts to generate a function-less isoform hTERT-s in PrCa, suppressed both telomerase activity and subsequent telomere shortening. RBM10 expression is negatively associated with PrCa progression. Gain or loss of RBM10 also significantly changed PrCa cell proliferation in vitro and in xenografts. RNA-IP and RNA pull-down assays reveal that RBM10 promotes the exclusion of exons7 and 8 which results in the production of TERT-s transcripts. This study may increase knowledge about potentially targetable cancer associated splicing factors and provide novel insights into therapeutic approach in PrCa.

Keywords: Alternative RNA splicing, RBM10, pancreatic cancer, hTERT

Introduction

Telomerase is an enzyme that is responsible for the maintenance of telomeres. Reactivation of telomerase has been universally recognized as a hallmark of cancer [1, 2]. Function as the telomerase catalytic subunit, telomerase reverse transcriptase (hTERT) is recognized as one of the key factors that control telomerase activity and maintain telomers in in up to 90% of cancers [1, 3]. Expression of hTERT was tight modulated at all levels including genomic and epigenomic alteration, alternative splicing and translational modification [4-6]. Expression regulation of hTERT at transcription level has been extensively explored. However, accumulating evidence suggest that transcriptional regulation is not sufficient to fully control telomerase activity [7]. Even though TERT gene transcription increased alongside aging, neither change of telomerase activity or full-length hTERT (hTERT-FL) transcripts containing the functional domain were detected, suggesting alternative splicing, may also participated in regulating telomerase activity [8, 9].

The hTERT gene consists of 16 exons and can generate several variants by RNA splicing [8]. Under certain circumstances, the exons 7 and 8 were excluded which lead to a reading frame shift and a premature stop codon within exon 10. This process results in translation of a truncated variant hTERT-s (also known as +α-β or minus beta) [9, 10]. Exons 5-9 were encoded for part of the reverse transcriptase domain of hTERT, so that the telomerase activity of hTERT-s was straightly suppressed [8, 9]. The hTERT-s has been reported to be downregulated in different type of cancers such as non-small cell lung cancer, oven cancer, prostate cancer, colorectal cancer and brain cancer [11-15]. While consensus on the role of the reverse transcriptase domain in regulating telomerase activity has been widely reached, mechanism that controlling alternative splicing that generates the inactive hTERT-s isoform is still not fully

studied. Through alternative splicing, most TERT transcripts are inactive variants instead of hTERT-FL in human. This mechanism ensures homeostasis of somatic cell and allows for human to have lower cancer incidence [16]. Deciphering the potential mechanisms that govern hTERT splicing is critical for better understanding of human cancer.

Alterative splicing of hTERT is known to be dysregulated in PrCa [17, 18]. Recently, several splicing factors were identified to potentially control hTERT splicing [11, 19]. RBM10, also called S1-1, is an RNA-binding protein which preferentially binds to GGU sequences and participates in alternative splicing [20-22]. RBM10 has been reported as a cancer-suppress gene through modulating NUMB and CREBBP splicing [23, 24]. Loss-of-function mutation of RBM10 is associated with high pancreatic tumor grade and lymphnode metastasis [25]. Since RBM10 is recognized as a tumor suppressor, and the regulation of RNA splicing is a crucial process that is aberrant in PrCa, we set out to confirm if hTERT splicing is regulated by RBM10 in pancreatic tumor.

In this study, we proposed an unveiled function of RBM10 that regulates hTERT splicing by binding to the GGU motif of PrCa cells to repress the production of hTERT-FL. Loss of RBM10 promote PrCa cell proliferation, invasion and xenograft growth. Our research provides a novel insight of how hTERT splicing is regulated in PrCa and a new direction for therapeutic approach targeting telomerase repression that may contribute to continuously PrCa inhibition.

Material and methods

Pancreatic TMA construction and pathology evaluation

Pancreatic ductal tumor samples were retrieved from The General Hospital of Western Theater Command of PLA and used to build tissue micro arrays (TMA). This TMA is consisting of tissue cores from 80 primary pancreatic ductal cancer patients.

RNA in situ hybridization (RISH) analyses

The hTERT-FL specific probe (detecting the junction region of exons 6 and 7 of hTERT-FL mRNA) and the hTERT-s specific probe (detecting the junction region of exons 6 and 9 of hTERT-s mRNA) were synthesized by Advanced Cell Diagnostic (Hayward, USA). RISH assays were performed using the BaseScope assay kit (Hayward, USA) following manufacture's protocol.

RISH signal was evaluated and scored as zero if there is no signal within the whole tissue core; one if signal is observed in less than 30% of the cell within a core; two if signal is observed in 30-60% of the whole tissue core and three if signal is observed in more than 60% of the whole tissue core.

Immunohistochemistry (IHC) analyses

The RBM10 antibody (PA5-83253, ThermoFisher scientific) was used for IHC staining. Stained TMA were scanned and digital images were generated by the Leica SCN400 scanner. IHC scores of RBM10 (0-3) was calculated by staining intensity (no as 0, low as 1, medium as 2, and high as 3) timed by the portion of RBM10 staining positive cells (0-100%). IHC scores ≥1.5 are recognized as high expression.

Cell lines

All PrCa cell lines (AsPX-1, BxPC-1, HPAC, PANC-1, CFPAC-1) and pancreatic ductal epithelial cell HPDE were purchased from ATCC and cultured at in 5% CO_2 37°C in DMEM medium containing 10% fatal bovine serum (HyClone, Logan, UT).

Western blot

Protein lysates of indicated cells were extracted by the lysis buffer (50 mM Tris, 1% NP40, 150 mM NaCl, 0.5% sodium deoxycholate, 0.1% SDS pH8.0 and proteinase inhibitors). The protein concentration was measured by BCA assay (Pierce). Total protein was separated on SDS polyacrylamide electrophoresis pages and then transferred to PVDF membranes. RBM10 antibody (PA5-83253, ThermoFisher scientific) was used for protein detection. Beta-actin (ab8227, Abcam) was used as loading control.

Reverse-transcription and realtime-qPCR

Total cell RNA was isolated by TRIZOL reagent. Deoxyribonuclease was used to clean DNA resident. Reverse transcription was carried out with superscript III (Invitrogen) and random hexamers according to the manufacture's instruc-

tion. Real-time qPCR was performed using the FastStart Universal SYBR Green Master mix (Roche) and run on the ABI 7900 HT system. All real-time qPCR results were from three independent experiment.

Construction of PrCa cell lines by lentivirus

Lentiviral vector encoding RBM10 and shRBM10 were purchased from Addgene and combined with VSVG and R8.9 vectors to package lentivirus and infect PCNA-1 cells. All cell lines were selected using blasticidin or puromycin. Expression or knockdown of RBM10 were confirmed by Western blot and real-time PCR

Cell proliferation, invasion and colony formation assays

The MTS regent was used for cell proliferation assay according to the manufacture's instruction. Cell proliferation rates were calculated as relative fold change of OD490 and normalized to the start point.

Bromodeoxyuridine (BrdU) assay was carried out following the manufacturer's instructions. Briefly, 1/500 diluted BrdU was added in 10^4 cells and incubated for 16 hours. Then, diluted anti-BrdU antibody was used to detect the BrdU following the manufacturer's instructions. The plates were washed and added TMB peroxidase substrate. Plates were read by the densitometer at the wavelength of 450 nm. BrdU index was calculated as relative fold change in OD450 and normalized to the control group.

Cell invasion was determined by transwell assays. Briefly, PCNA-1 cells were cultured in serum-free media overnight prior to planting into the Boyden chamber. The Matrigel-coated transwell filters were rehydrated. Cells were suspended and planted into the top chamber with serum-free culture media. The containing DMEM media containing 2% serum was filled into the bottom chamber. Cells were incubated overnight and cells left in the upper chamber were eliminate. Invaded cells were fixed and stained for 10 minutes with crystal violet. Stained cell was observed under ×10 magnification. All chambers were performed in triplicates.

For colony formation assay, about 10^3 cells were collected in 0.375% Soft agar with basal media and overlaid on 0.75% Noble aga in triplicate. After 10 days of growth, colonies larger than 0.1 mm were counted and the average of the colony number was calculated. All chambers were performed in duplicates.

Pancreatic tumor xenograft assay

All animal protocols were reviewed and approved by the Animal Care and Use Committee of The General Hospital of Western Theater Command of PLA and conducted following the institutional guidelines. The 4-6 weeks old nude mice were used for xenograft transplantation. About 10^5 cells were injected subcutaneously into the hind flanks of the nude mice. Tumor volume was monitored one or two times per week and calculated as Length * $(\text{Width})^2$ * 0.562.

Droplet digital TRAP assay

PCNA-1 cells were lysed, diluted, and used for the telomerase extension reaction. After 40 minutes reaction, telomerase was inactive by heat. The reaction products were amplified by droplet digital PCR for 40 cycles. The signal was measured and droplets were scanned and counted by the QX200 droplet reader. Telomerase extension was calculated as products per cell equivalents.

Telomerase activity assay

The TeloTAGGG telomerase PCR ELISA kit was used to analyze telomerase activity following the manufacturer's instruction (Roche). Briefly, total protein collected from PCNA-1 cell and added into the reaction mixture to generated telomere product. The product was then amplified by PCR for 30 cycles. ELISA assays was used to detected the amplified products, and telomerase activity was measured as the arbitrary unit of OD450-OD690.

Telomere length analysis

The average telomeres length (terminal restriction fragment lengths) was determined by the stretch PCR using the telomerase activity detection kit following the manufacturer's instructions (TeloChaser, Toyobo Co. Ltd.). Briefly, samples were lysis and incubated under ice-cold for 30 minutes. Insoluble fraction of the cellular lysate was eliminated at 12,000 g and

4°C centrifuged for 20 minutes. The supernatant was collected and about 9 ug of protein was used for PCR detection. Telomeric repeats were produce at 37°C for 60 mins and then isolated, incubated at 90°C for 3 minutes and subjected to 30 cycles of PCR including 94°C for 30 seconds, 50°C for 30 seconds, and 72°C for 60 seconds. The amplified terminal restriction fragments were run on a 10% polyacrylamide gel and analyzed by Southern blot.

Construction of hTERT minigenes

The human genomic BAC clone was used as the template to construct the hTERT minigene. Exon 6-9 and their 300-400 bp flanking intron regions of the hTERT gene (NM_198253) were amplified by Platinum Taq DNA Polymerase High Fidelity (Invitrogen) and cloned into the expression vector. The hTERT-minigene with mutant were generated using the original hTERT-minigene as the template by the Q5 site-directed mutagenesis kit (New England Biolabs). Sanger sequencing was used to confirmed the integrity of all the minigenes.

RNA immunoprecipitation (RNA-IP) assays

PCNA-1 cell transfected with Flag-RBM10 plasmid for 48 hours. Cell chromatin were cross-linked with formaldehyde for 20 minutes at 37°C. Cells were then cracked by sonication in RNA IP buffer (1% SDS, 50 mM Tris, and 10 mM EDTA, pH 8.0, plus protease inhibitor cocktail). Purified chromatin sample was added into 2 ug of Flag or control IgG antibody and incubated overnight at 4°C for immunoprecipitation. Target complex were precipitated by protein A/G agarose beads. Eluting buffer containing 1% SDS, 0.1 M $NaHCO_3$, and 50 µl RNase inhibitor was used to elute immunocomplexes. Cross-links was reversed by adding 10 µl 5 M NaCl into 500 µl of eluted immunocomplexes and heated for 2 hours at 64°C. Immunoprecipitated RNA fragments were eluted by 1500 ul lysis buffer containing 1% 2-mercaptoenthanol. Purelink RNA Mini Kit was used to isolate eluted RNA and subsequence to reverse transcription. DNA products were quantified by real-time qPCR and presented as percentage of input.

RNA pull-down assay

NETN buffer with proteinase inhibitor cocktail were used to lysis PCNA-1 cells transfected with Flag-RBM10 plasmid. Biotin-labeled RNA oligos were attached onto streptavidin beads at 4°C for 2 hours. Cell lysate was incubated combined with beads banded the biotin-labeled RNA oligos to pull-down the Flag-RBM10 protein. Purified proteins were detected by Western blot using anti-Flag antibody.

Statistics

Statistical analysis was carried out by the GraphPad Prism 8.0 software. Differences among groups were compared by one-way ANOVA test. Spearman correlation analysis was used to evaluate the correlation between hTERT-FL and hTERT-s RISH scores with tumor stage. The level of significance was set at $P<0.05$ as *, $P<0.01$ as **.

Results

Downregulation of RBM10 expression associates poor prognosis of PrCa

To explore the potential factors associated with hTERT splicing and PrCa progression, we analyzed the published hTERT minigene siRNA screen [11] results and significantly altered gene in two PrCa database (TCGA and GTEx) [26, 27]. RBM10 was one of the top-ranking PrCa specific RNA-binding protein that associated with alternative splicing of hTERT and PrCa progression (**Figure 1A**). Genomic profiling of PrCa patients (GEPIA) showed that among PrCa patients, RBM10 expression was negatively correlated with tumor stage (**Figure 1B**). Patients with relatively lower RBM10 expression have shorter total patient survival and disease-free survival duration (**Figure 1C**). Similar results were also obtained from data of TCGA PanCancer atlas (**Figure 1D**). In cell model, RBM10 expressed differently in several pancreatic cell lines, all PrCa cell lines expressed lower levels of RBM10 than the benign HPDE cells (**Figure 1E**). Reduced RBM10 protein levels in PrCa cell lines were correlated with increased levels of hTERT-FL mRNA, but decreased hTERT-s mRNA levels (**Figure 1F**).

We further utilized IHC assays on TMAs to measure RBM10 expression in our PrCa cohort (**Figure 2A**, **2B**). Consistent with RBM10 mRNA results, our IHC results indicated that patients with relatively lower RBM10 protein expression have shorter total patient survival and disease-free survival rates (**Figure 2C**). RBM10 IHC score was also negatively correlated with tumor stage (**Figure 2D**). In addition, the mean RBM10

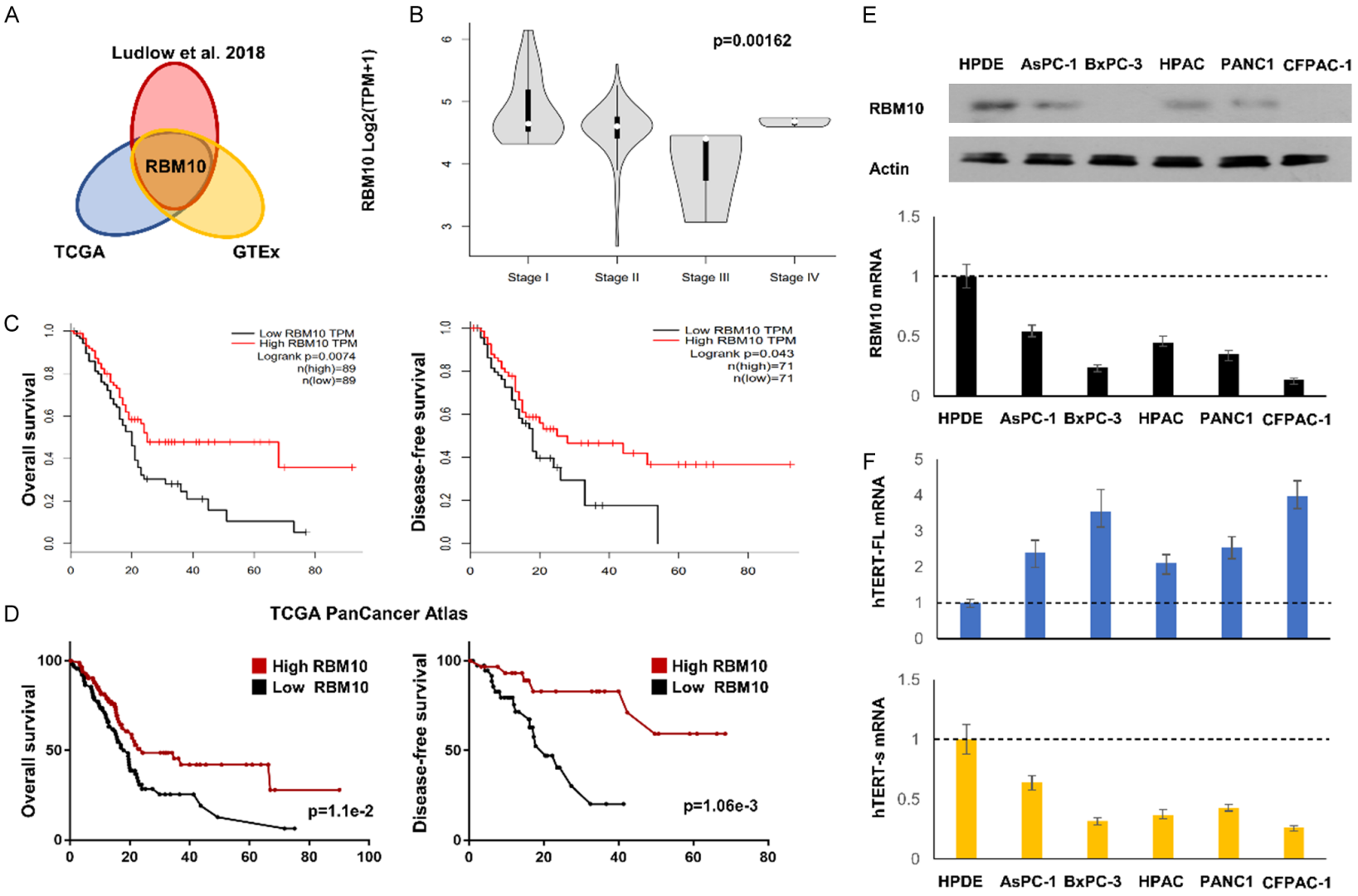

Figure 1. RBM10 expression in PrCa(PrCa) patients and cell models. A. A Venn diagram of results from indicated database shows splicing factor RBM10 is significantly upregulated in PrCa. B. Whole transcriptome sequencing data from TCGA and GTEx database were analyzed in the GEPIA website (http://gepia.cancer-pku.cn/). RBM10 mRNA level was present as Log2(TPM+1) and used to compare compared RBM10 mRNA levels among different pancreatic tumor stage. C. Overall survival and disease-free survival of pancreatic patients by RBM10 level were compared and analyzed by Kaplan-Meier curves. D. Whole transcriptome sequencing data from TCGA PanCancer Atlas database were analyzed in the cbioportal website (http://www.cbioportal.org/). Z-scores were used to divide PrCa patients into RBM low and high groups. Overall survival and disease-free survival of pancreatic patients by RBM10 level were compared and analyzed by Kaplan-Meier curves. E. Multiple pancreatic cell lines were used to measure RBM10 expression by immunoblotting and realtime-qPCR. F. Multiple pancreatic cell models were used

to analyze hTERT-FL and hTERT-s expression by real-time PCR. Original, full-length blot images were provided in Supplementary Figure 1.

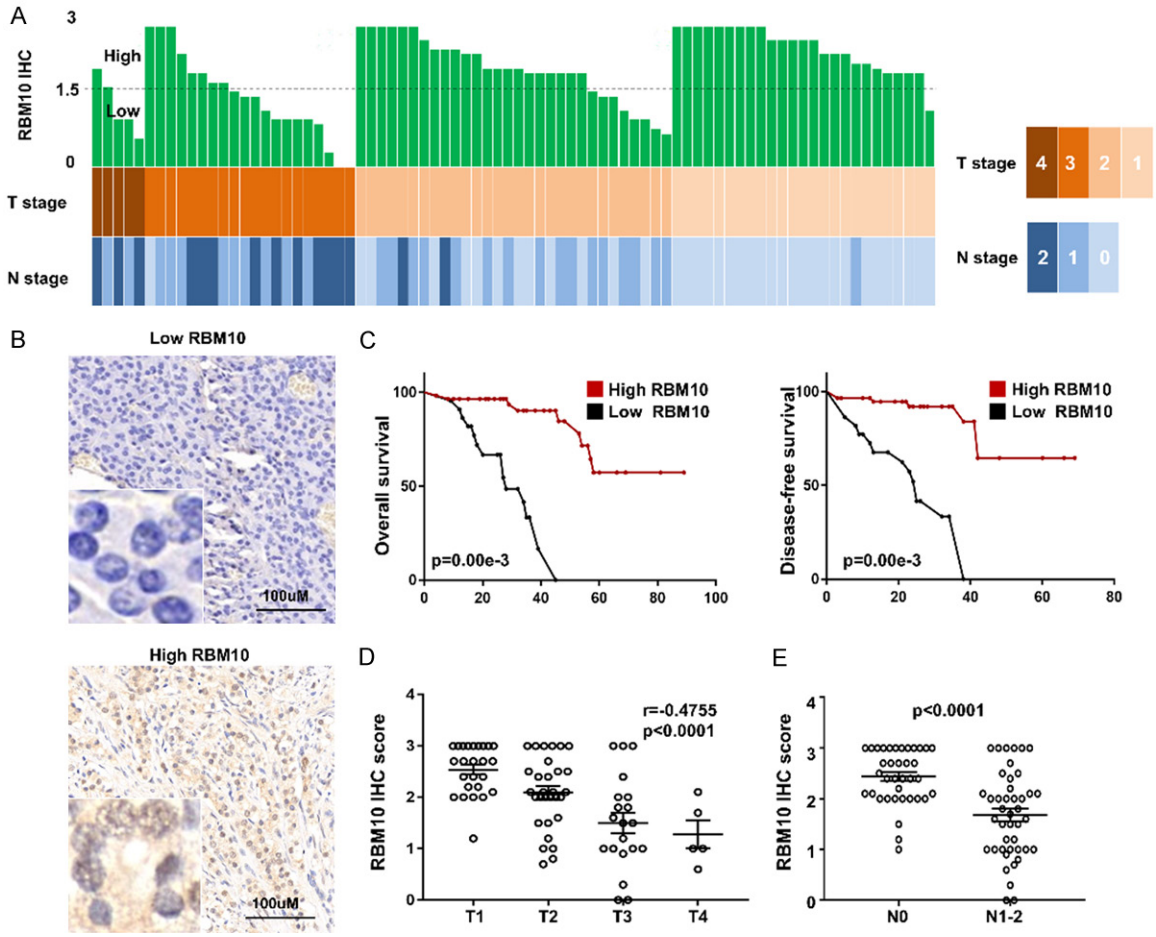

Figure 2. Application of TMA to study RBM10 expression during PrCa progression. A, B. RBM10 IHC assays were carried out on the PrCa TMA using RBM10 antibody as described in the Methods section. Representative images of RBM10 IHC staining are shown. IHC scores were used to divide PrCa patients into RBM10 low (less than 1.5) and high (higher or equal to 1.5) groups. C. Overall survival and progression-free survival of pancreatic patients were plotted by RBM10 IHC score using Kaplan-Meier curves. D. Scattered plots show RBM10 IHC scores of indicated tumor groups. The association of RBM10 level with PrCa tumor stage was calculated by Spearman's correlation test. E. RBM10 expression in tumor with or without LNs metastasis were compared by t-test.

IHC score was higher in patient without lymphoid metastasis but decreased in patient with lymphoid metastasis (**Figure 2E**). In summary, both public data and our TMA results indicate that reduced RBM10 expression associates with advanced PrCa and poor patient survival.

RBM10 regulates telomerase activity in PrCa cells

Lentivirus vectors stably expressing RBM10 or shRBM10 RNA were used to infect PCNA-1 cell. Telomere length assay showed that RBM10 overexpression reduced and RBM10 depletion enhanced PCNA-1 telomere length (**Figure 3A**). Consistently, gain- or loss-of-function of also altered PCNA-1 telomerase activity (**Figure 3B**, **3C**). Furthermore, transfection of hTERT-FL expression vector or shhTERT RNA were able to rescue the change of telomere length and telomerase enzyme induced by RBM10 alteration (**Figure 3D-F**). These results indicated RBM10 regulated telomerase activity in PrCa cells.

RBM10 suppresses PrCa cell growth and xenograft progression

MTS and BrdU assays showed that PCNA-1 cell proliferation rates were inhibited by gain-of-

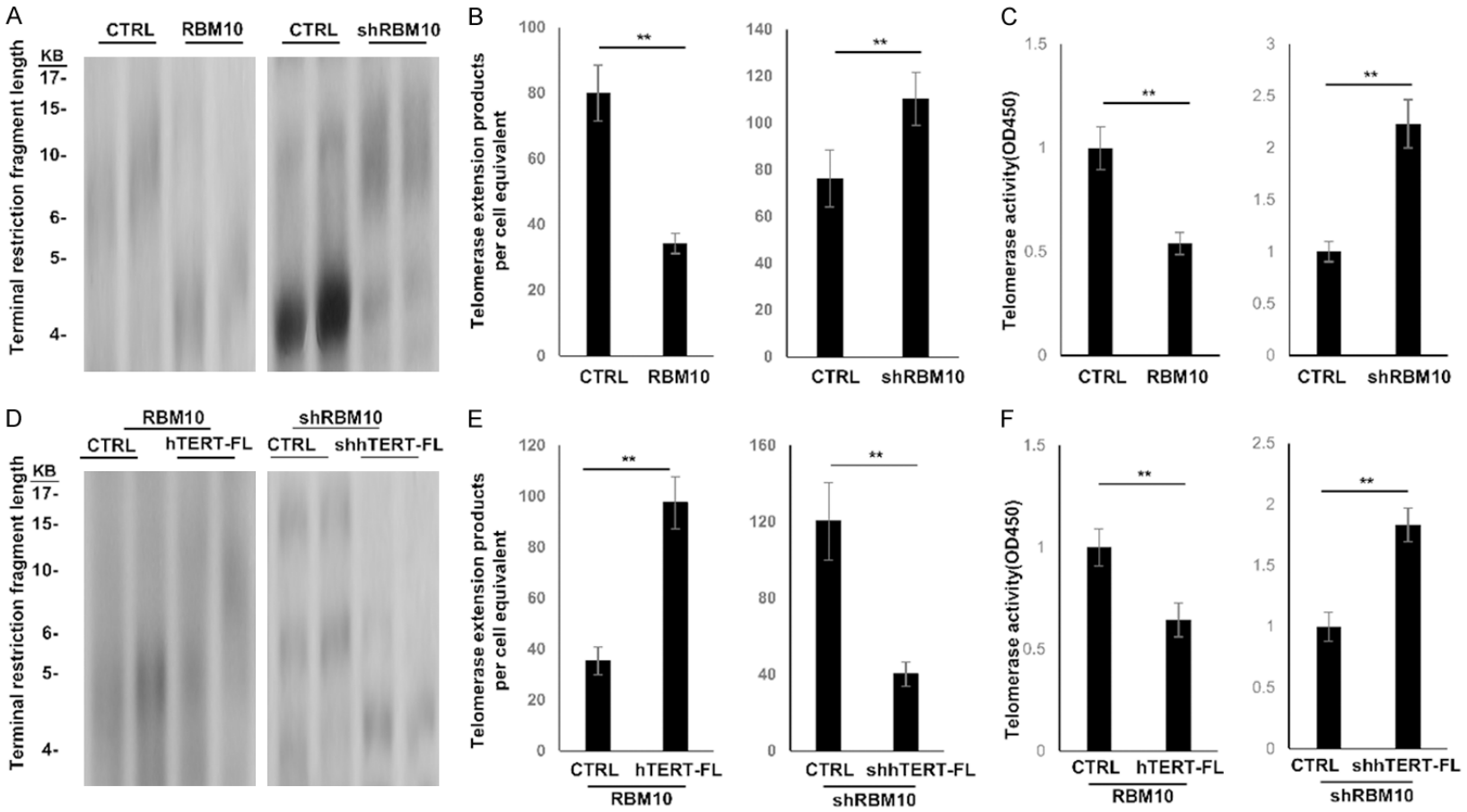

Figure 3. RBM10 inhibits telomerase activity in PrCa cells. (A-C) Gain- and loss-of-function of RBM10 was applied to PCNA-1 by lentivirus. (A) Terminal restriction fragment length analysis of indicated cells were analyzed using TRF-Southern blot. (B) Telomerase activity was measured by droplet digital TRAP (with about fifty cell equivalents) in indicated cells. (C) Telomerase activity was assayed and expressed as an arbitrary unit of absorbance at OD450-OD690 as described in the Material and Method section. (D-F) Telomerase activity alteration in (A-C) can be rescued by gain- and in RBM10 overexpression cells and by loss-of-function of hTERT-FL in RBM10 depletion cells. The experiment was repeated three times and presented as the mean ± SD, *P<0.05. Original, full-length gel images were provided in Supplementary Figure 2.

function of RBM10 and enhanced by RBM10 depletion. Consistently, these effects can also be abolished by introduction or depletion of hTERT-FL (**Figure 4A**, **4B**). Similar results were also found in PCNA-1 cell invasion and anchorage colony formation assays (**Figure 4C**, **4D**). Using the PCNA-1 xenograft model, we showed RBM10 inhibited and shRBM10 promoted PCNA-1 xenograft growth which can be rescued by introduction of hTERT-FL or shhTERT-FL (**Figure 4E**). These results indicate that RBM10 inhibits pancreatic cell proliferation, invasion, colony formation, and xenograft growth.

RBM10 expression is associated with hTERT splicing in PrCa

We found that hTERT-FL is expressed at merely low levels in normal pancreatic cell but dramatically induced in PrCa cell, while hTERT-s expression levels shows opposite trend (**Figure 1F**). To validate these findings, RNA in situ hybridization (RISH) assays were applied in our TMA (**Figure 5A**, **5B**) and confirmed that compared to RBM10 high tissues, hTERT-FL staining was higher in RBM10 low PrCa. hTERT-FL RISH signaling was scored as high (score =3) in 13.6% (3/22), moderate (score =2) in 68,2% (15/22), and low (score =1) in 13.6% (3/22) of RBM10 low samples. Only 4.5% (1/22) of RBM10 low were hTERT-FL negative. By contrast, none of RBM10 high sample strongly expressed hTERT-FL, 13.8% (8/58) expressed moderate, 69.0% (40/58) expressed weak and almost 17.2% (10/58) express no hTERT in RBM10 high tissue. Meanwhile, no high hTERT-s RISH scored was detected in RBM10 low samples, only 27.3% (6/22) of RBM10 low samples express moderate and 72.7(16/22) express weak hTERT-s (**Figure 5C**). Consistently, RBM10 IHC score was negatively correlated with hTERT-FL RISH score but positively correlated with hTERT-s RISH score (**Figure 5D**). Together, these results suggest a tightly association of RBM10 expression with hTERT splicing.

RBM10 interacts with hTERT pre-mRNA and inhibits exons inclusion

Since the RBM10 is an RNA binding protein and regulates hTERT-associated telomerase activity, we hypothesized that RBM10 directly regulates hTERT RNA splicing. RBM10 overexpression downregulated and shRBM10 up regulated hTERT-FL/hTERT-s mRNA ratio (**Figure 6A**, **6B**). The GGU motif has been reported to be a consensus RBM10 binding site. We found several GGU motif within the 5' splice site of exon 5-8 in hTERT gene. *In vivo* RNA immunoprecipitation assays confirmed that RBM10 was recruited to the sites next to the 5' splice sites of hTERT intron 7 and 8 (S4-S5 sites), but not others regions (**Figure 6C**). RNA pull-down assays indicated that RBM10 can directly bind to the wild type, but not the mutant GGU motif within S4 and S5 region in PCNA-1 cells (**Figure 6D**). To further confirm that RBM10 regulates hTERT splicing, we constructed an hTERT minigene vector in which exons 7/8 and their flanking 300-400 bp intron base pairs were inserted between exons 6 and 9 (**Figure 5C**). When transfected into PCNA-1 cell, RBM10 upregulated hTERT-s but downregulated hTERT-FL mRNA derived from the minigene vector. In addition, Site-specific mutagenesis (GGU to GAU) within the RBM10 binding sites showed repress of RBM10-mediated exon7/8 skipping (**Figure 6E**). These results confirm that RBM10 regulates hTERT splicing.

Discussion

The hTERT can be spliced into several different isoforms, but only hTERT-FL is able to produce catalytic protein component that is capable of maintain telomeres [28]. In our study, we found that PrCa express low levels of RBM10 were more advanced and have poor prognosis (**Figure 1**). Loss of RBM10 inhibits the exons 7 and 8 skipping during hTERT splicing to generate functional telomerase and maintain telomere length (**Figure 6**). Further, RBM10 regulates growth and invasion in PrCa cells, coupling telomere length maintenance.

Several cis elements play critical roles in hTERT splicing regulation. It has been reported that lack of cis elements of intron in hTERT pre-mRNA can prevent the inclusion of exon7 and 8 [11]. These cis elements are conserved in hTERT pre-mRNA and potentially allow hTERT to be alternative spliced by different splicing factors such as NOVA1, SRSF11, hnRNP H2, and hnRNP L [11, 29, 30]. RBM10 has a RanBP2-type Zn finger, which is capable of binding with high affinity to 5' splice site of exon7-8 in hTERT pre-mRNA with a GGU motif. Intriguingly, the 5' splice site of exon 7-8 has several GGU motifs (**Figure 6C**) which engage RBM10 binding and

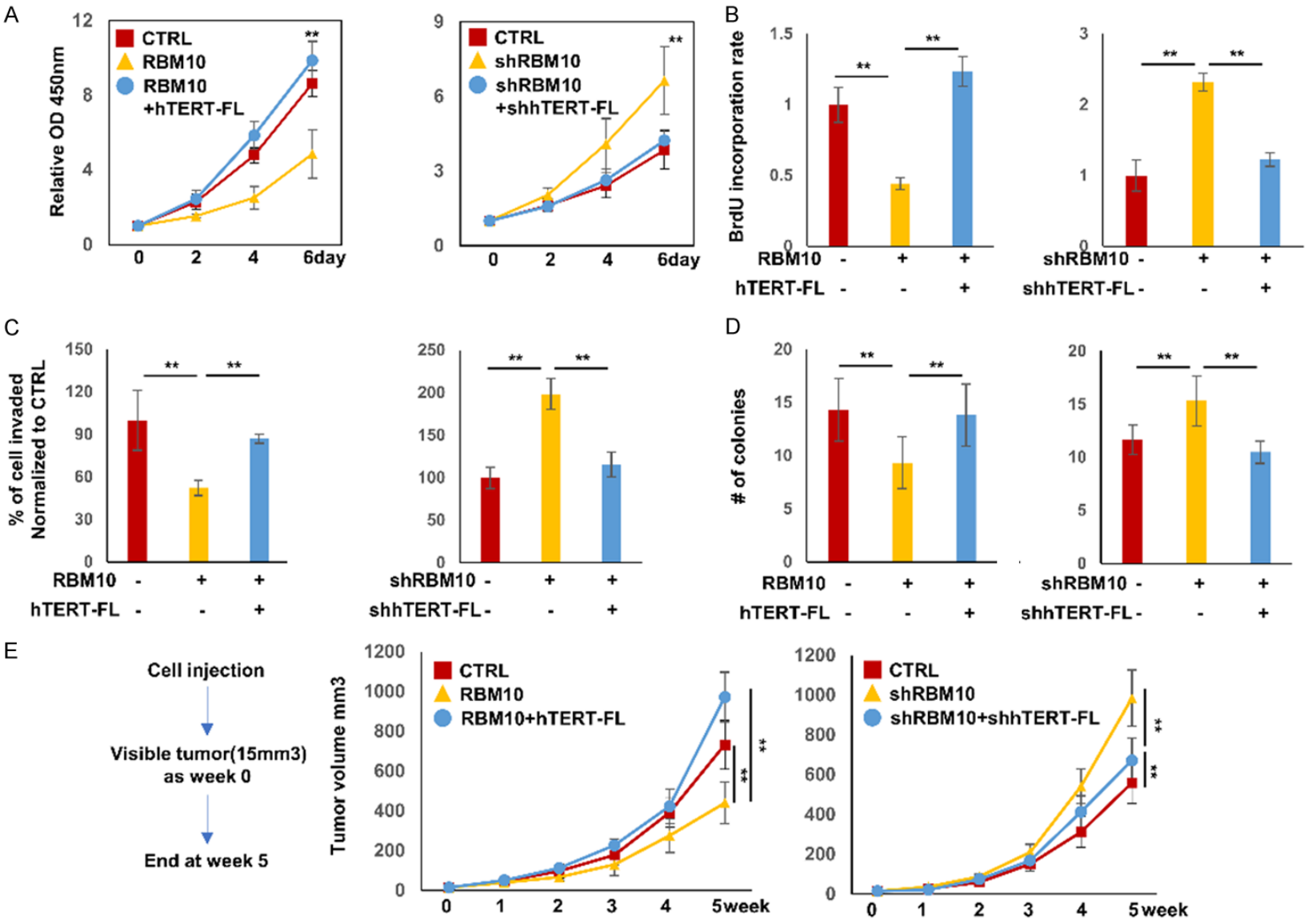

Figure 4. RBM10 inhibits PrCa cell proliferation, colony formation and xenograft growth. A-D. Gain- and loss-of-function of RBM10 with was applied to PCNA-1 cell and rescued by gain- and loss-of-function of hTERT-FL. A. Cell proliferation rate were analyzed by MTS assays and calculated as relative OD490 fold change to that at day 0. B. BrdU incorporation assays were performed and relative BrdU incorporation rate were present. C. Cell invasion rates were measured by trans-well assays. D. Colony formation of PCNA-1 cell were analyzed by soft agar assay and colony numbers were counted with diameters more than 100 um. E. PCNA-1 xenografts were established as described in the Methods section. Tumor volumes were measured weekly and plotted.

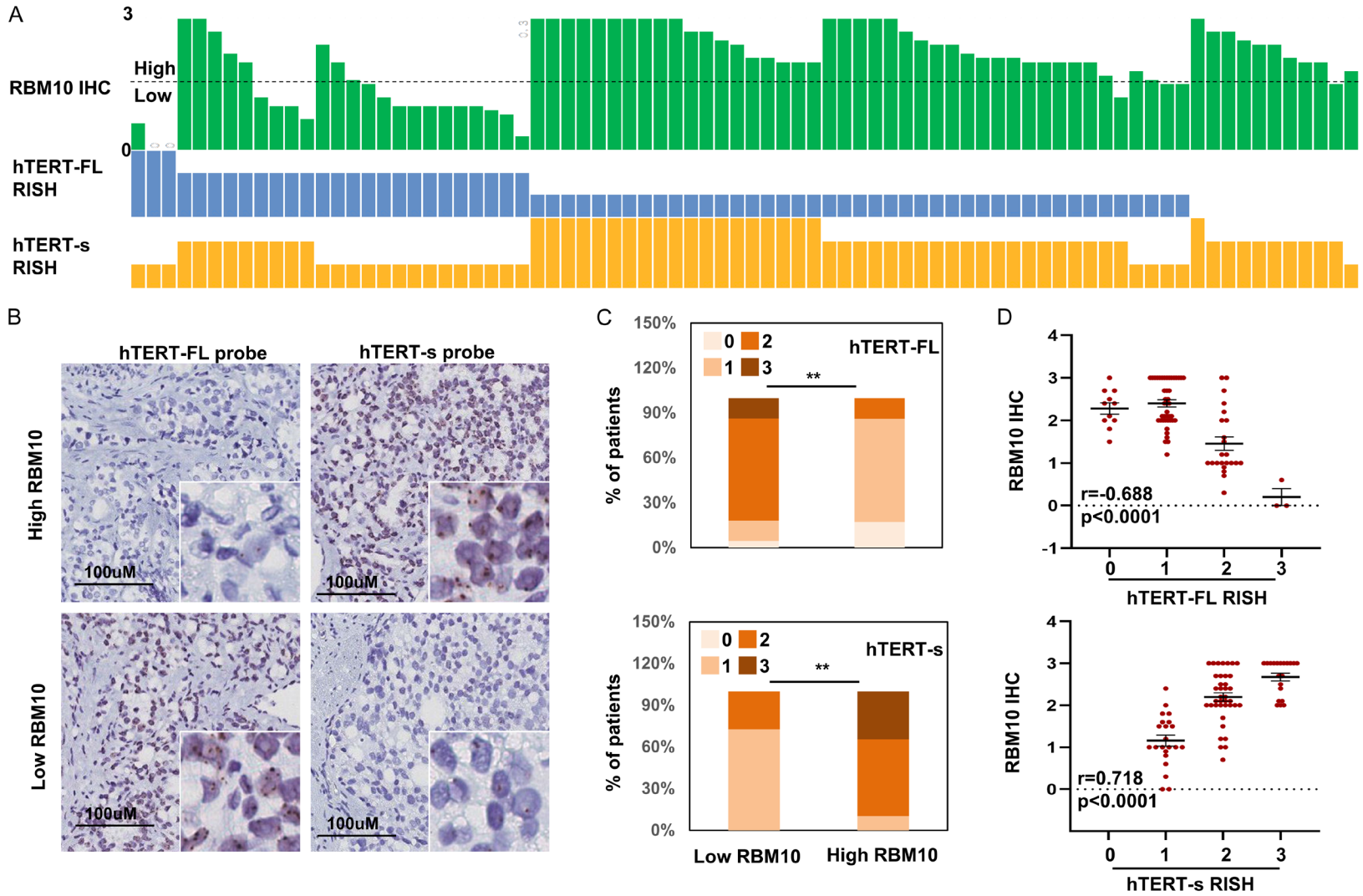

Figure 5. hTERT splicing variants expression in PrCa TMA. A, B. RISH assays were performed on PrCa TMA using hTERT-FL and hTERT-s probes as described in the Material and Method section, representative images were shown. C. Distribution of hTERT-FL and hTERT-s RISH scores in RBM10 low or high groups were plotted. D. hTERT-FL and hTERT-s expression in correlation with RBM10 IHC scores was analyzed by Spearman's correlation test. Results were calculated and presented as the mean ± SEM.

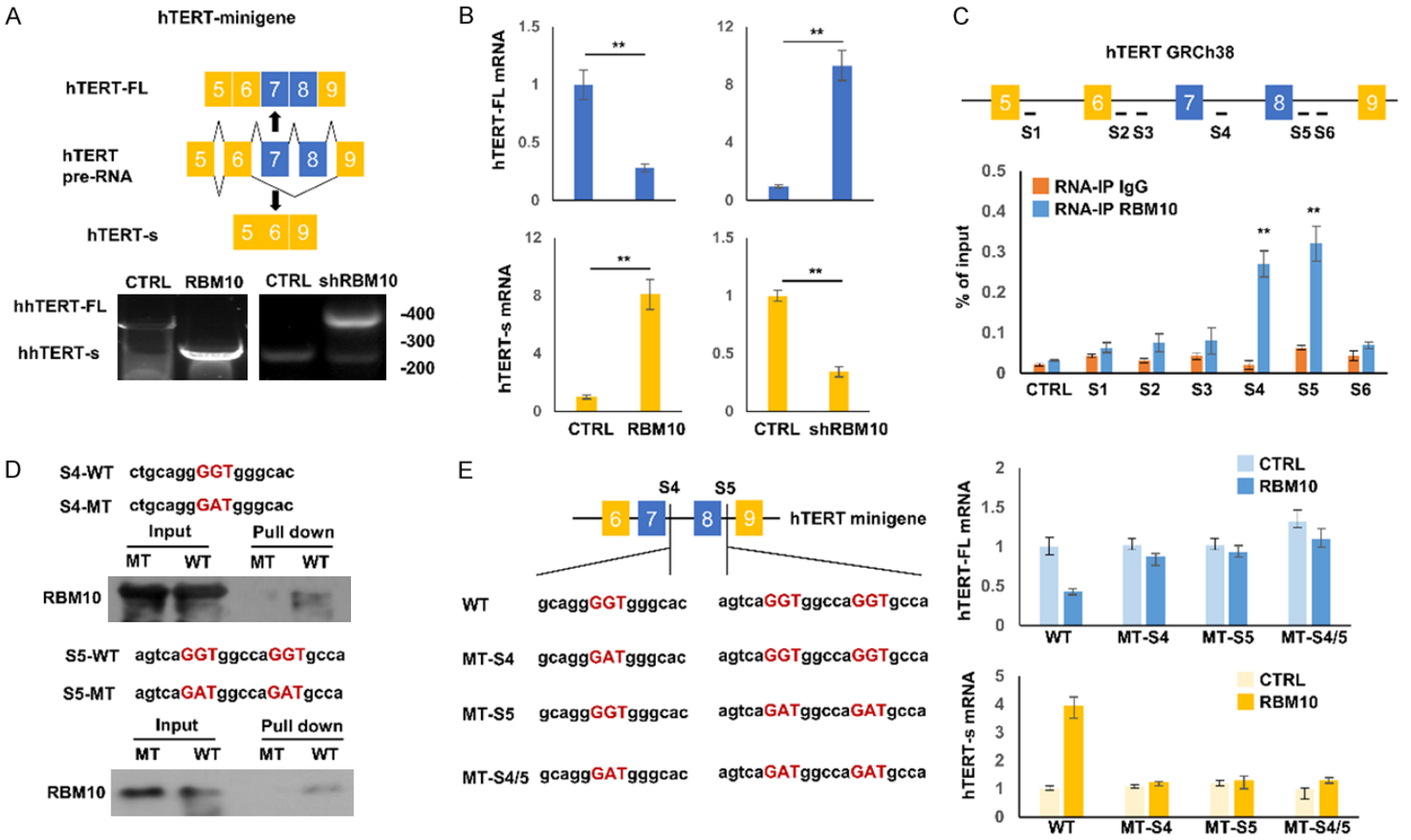

Figure 6. RBM10 binds to the GGU motif in hTERT precursor RNA and regulates hTERT splicing. (A, B) A schematic diagram shows the structure of the hTRET minigene reporter and the derived hTERT splice variants. Expression of hTERT-FL and hTERT-s in PCNA-1 cell with gain- and loss-of function of RBM10 was validated by (A) RT-PCR and (B) realtime-PCR. (C) A schematic diagram of the potential RBM10 binding sites (S1-S6) analyzed in RNA-IP assays. PCNA-1 cells were transfected with the Flag-RBM10 plasmid. *In vivo* RNA-IP were carried out using IgG or Flag antibody. Precipitated RBM10 associated RNA fragments were reversed into cDNA and analyzed by real-time qPCR. Level of precipitated RNA were presented as % of input. (D) Flag-RBM10 was pulldown by biotin-labeled oligos from PCNA-1 cells and detected by western blot using Flag antibody. (E) A schematic diagram presents the structure of hTERT minigene vector. PCNA-1 cells were transfected with control, wild or mutant hTERT-minigene in the presence of RBM10 plasmid or not. Total RNA was collected and hTERT-FL and hTERT-s mRNA levels were measured by realtime-qPCR. All experimental assays were repeated in three independent experiments. Data were presented as the mean ± SD ** delegates P<0.01 when comparing with controls. Original, full-length blot images were provided in Supplementary Figures 3 and 4.

consequently blocking the site for splicing and inducing exon 7-8 skipping. This hypothesis is supported by the results that RBM10 were observed to potentially bind hTERT pre-mRNA and inhibits hTERT-FL transcript generation (**Figure 6**). In our research, we proposed a model for how RBM10 protein interacted with hTERT pre-mRNA. In this model, we propose that RBM10 binds to GGU motifs within the 5' splice site of intron 7-8 and brings the 5' splice site of exon 6 in close proximity to the 3' splice site of exon 9, generating hTERT-s mRNAs with exon 7 and 8 skipping. Supporting this model, RBM10 failed to bind to the hTERT minigene bearing site-mutant of GGU motif and PCNA-1 cell transfected with site-mutant minigene switched their splicing pattern to almost solely hTERT-s (**Figure 6E**).

Since RBM10 regulates hTERT splicing and suppress hTERT-FL expression, downregulation of RBM10 genes in PrCa is predicted to maintain telomere length and likely switch on cell mitosis and proliferation. This hypothesis is consistent with our findings that RBM10 depletion suppresses PrCa cell growth and tumor progression (**Figure 4**). Although a whole-exome sequencing research showed loss-of-function mutation of RBM10 was associated with long survival [25], it does rule out the possibility that other mechanisms contributes to RBM10 function since only 4% tumors bearing indicated mutation. Our research show that low RBM10 expression level in both TCGA and our cohorts is associated with advanced pancreatic tumor stage and poor prognosis (**Figures 1**, **2**). These findings support the idea that RBM10 is a tumor-suppress gene which represses tumor development and progression by modulating hTERT splicing. Also, as a well-known RNA binding protein, RBM10 may also have functions other than regulating splicing [31]. Our results point out the possibility that by targeting RBM10 expression and function, telomerase activity and telomere length maintenance in PrCa can be manipulated which may be a novel therapeutic intervention.

The mechanisms of downregulation of RBM10 in pancreatic remain unknown. No cancer-specific promoter mutations were reported in PrCa [32]. Only 4% pancreatic tumors were reported to bearing loss-of-function mutation of RBM10 [25]. Thus, suppression of RBM10 may involve epigenetic mechanisms including histone post-translational modifications. We did not profile RBM10 mutation or other RBM10 genomic-or epigenomic alterations in our cohort. However, regardless of these that prevent us from establishing a full model that explain the association between RBM10 and PrCa, they did not impede us from drawing the conclusion that RBM10 appears to integrate hTERT alternative splicing with sustained tumor progression. Thus, our study has provided a new insight into splicing regulation of hTERT in PrCa and identified RBM10 as a candidate gene for manipulating the hTERT splicing machinery for PrCa therapy.

Acknowledgements

This study was supported by the following foundations: Science & Technology Department of Sichuan Province (2018SZ0033 to XW), Sichuan Traditional Chinese Medicine Administration (2018QN050 to XW, 2018HJZX013 to YH), the National Natural Science Foundation of China (81402507 to WH, 81900339 to JH).

Disclosure of conflict of interest

None.

Address correspondence to: Yonghe Hu and Jun Hou, Department of Pharmacy, The General Hospital of Western Theater Command of PLA, No 270 Rongdu Road, Jinniu District, Chengdu 610083, China. Tel: +86-28-86570825; Fax: +86-28-86570825; E-mail: huyonghezyy@163.com (YHH); jun_hou@yeah.net (JH)

References

[1] Kim NW, Piatyszek MA, Prowse KR, Harley CB, West MD, Ho PL, Coviello GM, Wright WE, Weinrich SL and Shay JW. Specific association of human telomerase activity with immortal cells and cancer. Science 1994; 266: 2011-2015.

[2] Hanahan D and Weinberg RA. Hallmarks of cancer: the next generation. Cell 2011; 144: 646-674.

[3] Cohen SB, Graham ME, Lovrecz GO, Bache N, Robinson PJ and Reddel RR. Protein composition of catalytically active human telomerase from immortal cells. Science 2007; 315: 1850-1853.

[4] Bell RJ, Rube HT, Xavier-Magalhaes A, Costa BM, Mancini A, Song JS and Costello JF. Understanding TERT promoter mutations: a common path to immortality. Mol Cancer Res 2016; 14: 315-323.

[5] Wong MS, Wright WE and Shay JW. Alternative splicing regulation of telomerase: a new paradigm? Trends Genet 2014; 30: 430-438.
[6] Idilli AI, Pagani F, Kerschbamer E, Berardinelli F, Bernabe M, Cayuela ML, Piazza S, Poliani PL, Cusanelli E and Mione MC. Changes in the expression of pre-replicative complex genes in hTERT and ALT pediatric brain tumors. Cancers (Basel) 2020; 12: 1028.
[7] Kim W, Ludlow AT, Min J, Robin JD, Stadler G, Mender I, Lai TP, Zhang N, Wright WE and Shay JW. Regulation of the human telomerase gene TERT by telomere position effect-over long distances (TPE-OLD): implications for aging and cancer. PLoS Biol 2016; 14: e2000016.
[8] Hrdlickova R, Nehyba J and Bose HR Jr. Alternatively spliced telomerase reverse transcriptase variants lacking telomerase activity stimulate cell proliferation. Mol Cell Biol 2012; 32: 4283-4296.
[9] Yi X, Shay JW and Wright WE. Quantitation of telomerase components and hTERT mRNA splicing patterns in immortal human cells. Nucleic Acids Res 2001; 29: 4818-4825.
[10] Yi X, White DM, Aisner DL, Baur JA, Wright WE and Shay JW. An alternate splicing variant of the human telomerase catalytic subunit inhibits telomerase activity. Neoplasia 2000; 2: 433-440.
[11] Ludlow AT, Wong MS, Robin JD, Batten K, Yuan L, Lai TP, Dahlson N, Zhang L, Mender I, Tedone E, Sayed ME, Wright WE and Shay JW. NOVA1 regulates hTERT splicing and cell growth in non-small cell lung cancer. Nat Commun 2018; 9: 3112.
[12] Brambilla C, Folini M, Gandellini P, Daprai L, Daidone MG and Zaffaroni N. Oligomer-mediated modulation of hTERT alternative splicing induces telomerase inhibition and cell growth decline in human prostate cancer cells. Cell Mol Life Sci 2004; 61: 1764-1774.
[13] Alsiary R, Brownhill SC, Bruning-Richardson A, Hutson R, Griffin N, Morrison EE, Bond J, Burchill SA and Bell SM. Expression analysis of the MCPH1/BRIT1 and BRCA1 tumor suppressor genes and telomerase splice variants in epithelial ovarian cancer. Gene 2018; 672: 34-44.
[14] Jeung HC, Rha SY, Shin SJ, Ahn JB, Park KH, Kim TS, Kim JJ, Roh JK and Chung HC. Changes in telomerase activity due to alternative splicing of human telomerase reverse transcriptase in colorectal cancer. Oncol Lett 2017; 14: 2385-2392.
[15] Khajehgoodari R, Khorvash F, Kheirollahi M, Mirsafaie M and Salehi M. Correlations between the expression of hTERT and alpha and beta splice variants in human brain tumors. Adv Clin Exp Med 2019; 28: 507-513.
[16] Aviv A, Anderson JJ and Shay JW. Mutations, cancer and the telomere length paradox. Trends Cancer 2017; 3: 253-258.
[17] Hayes GM, Carrigan PE, Beck AM and Miller LJ. Targeting the RNA splicing machinery as a novel treatment strategy for pancreatic carcinoma. Cancer Res 2006; 66: 3819-3827.
[18] Gansauge F, Gansauge S, Zobywalski A, Scharnweber C, Link KH, Nussler AK and Beger HG. Differential expression of CD44 splice variants in human pancreatic adenocarcinoma and in normal pancreas. Cancer Res 1995; 55: 5499-5503.
[19] Sayed ME, Yuan L, Robin JD, Tedone E, Batten K, Dahlson N, Wright WE, Shay JW and Ludlow AT. NOVA1 directs PTBP1 to hTERT pre-mRNA and promotes telomerase activity in cancer cells. Oncogene 2019; 38: 2937-2952.
[20] Collins KM, Kainov YA, Christodolou E, Ray D, Morris Q, Hughes T, Taylor IA, Makeyev EV and Ramos A. An RRM-ZnF RNA recognition module targets RBM10 to exonic sequences to promote exon exclusion. Nucleic Acids Res 2017; 45: 6761-6774.
[21] Sun Y, Bao Y, Han W, Song F, Shen X, Zhao J, Zuo J, Saffen D, Chen W, Wang Z, You X and Wang Y. Autoregulation of RBM10 and cross-regulation of RBM10/RBM5 via alternative splicing-coupled nonsense-mediated decay. Nucleic Acids Res 2017; 45: 8524-8540.
[22] Inoue A, Takahashi KP, Kimura M, Watanabe T and Morisawa S. Molecular cloning of a RNA binding protein, S1-1. Nucleic Acids Res 1996; 24: 2990-2997.
[23] Hernandez J, Bechara E, Schlesinger D, Delgado J, Serrano L and Valcarcel J. Tumor suppressor properties of the splicing regulatory factor RBM10. RNA Biol 2016; 13: 466-472.
[24] Wang Y, Gogol-Doring A, Hu H, Frohler S, Ma Y, Jens M, Maaskola J, Murakawa Y, Quedenau C, Landthaler M, Kalscheuer V, Wieczorek D, Wang Y, Hu Y and Chen W. Integrative analysis revealed the molecular mechanism underlying RBM10-mediated splicing regulation. EMBO Mol Med 2013; 5: 1431-1442.
[25] Witkiewicz AK, McMillan EA, Balaji U, Baek G, Lin WC, Mansour J, Mollaee M, Wagner KU, Koduru P, Yopp A, Choti MA, Yeo CJ, McCue P, White MA and Knudsen ES. Whole-exome sequencing of pancreatic cancer defines genetic diversity and therapeutic targets. Nat Commun 2015; 6: 6744.
[26] Tang Z, Li C, Kang B, Gao G, Li C and Zhang Z. GEPIA: a web server for cancer and normal gene expression profiling and interactive analyses. Nucleic Acids Res 2017; 45: W98-W102.
[27] Blum A, Wang P and Zenklusen JC. SnapShot: TCGA-analyzed tumors. Cell 2018; 173: 530.

[28] Wong MS, Chen L, Foster C, Kainthla R, Shay JW and Wright WE. Regulation of telomerase alternative splicing: a target for chemotherapy. Cell Rep 2013; 3: 1028-1035.
[29] Listerman I, Sun J, Gazzaniga FS, Lukas JL and Blackburn EH. The major reverse transcriptase-incompetent splice variant of the human telomerase protein inhibits telomerase activity but protects from apoptosis. Cancer Res 2013; 73: 2817-2828.
[30] Lee JH, Jeong SA, Khadka P, Hong J and Chung IK. Involvement of SRSF11 in cell cycle-specific recruitment of telomerase to telomeres at nuclear speckles. Nucleic Acids Res 2015; 43: 8435-8451.
[31] Mohan N, Kumar V, Kandala DT, Kartha CC and Laishram RS. A splicing-independent function of RBM10 controls specific 3'UTR processing to regulate cardiac hypertrophy. Cell Rep 2018; 24: 3539-3553.
[32] Seiler M, Peng S, Agrawal AA, Palacino J, Teng T, Zhu P, Smith PG; Cancer Genome Atlas Research Network, Buonamici S and Yu L. Somatic mutational landscape of splicing factor genes and their functional consequences across 33 cancer types. Cell Rep 2018; 23: 282-296, e284.

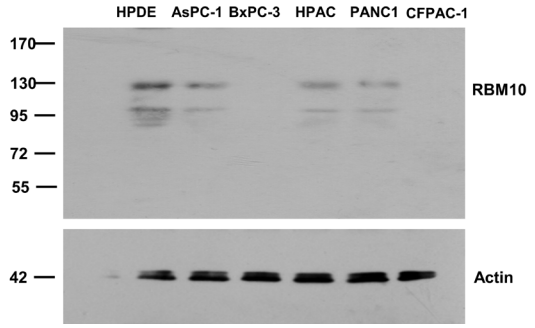

Supplementary Figure 1. Multiple pancreatic cell lines were used to measure RBM10 expression by immunoblotting and realtime-qPCR (Original image of **Figure 1E**).

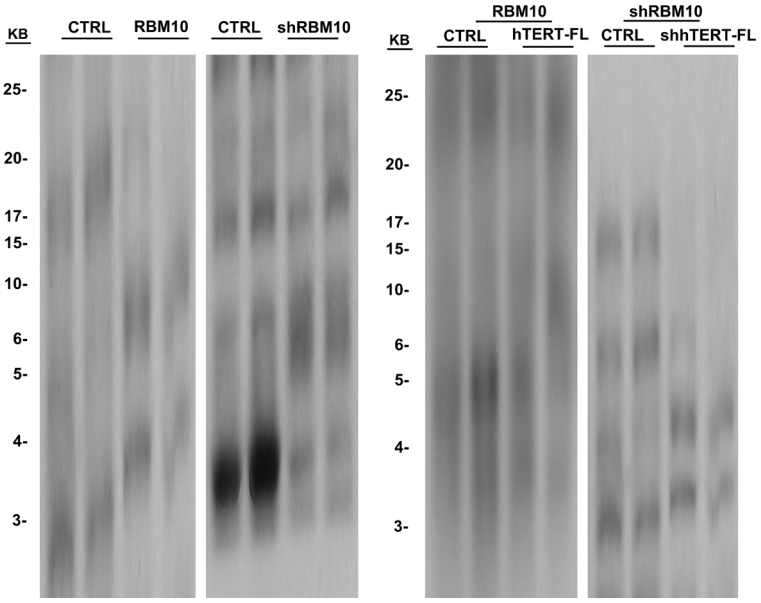

Supplementary Figure 2. Terminal restriction fragment length analysis of indicated cells were analyzed using TRF-Southern blot (Original image of **Figure 3A** and **3D**).

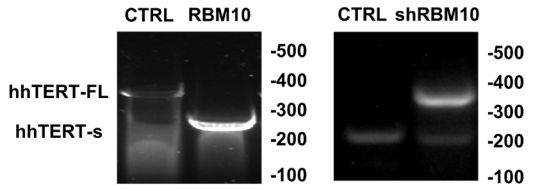

Supplementary Figure 3. Expression of hTERT-FL and hTERT-s in PCNA-1 cell with gain- and loss-of function of RBM10 was validated by RT-PCR (Original image of **Figure 6A**).

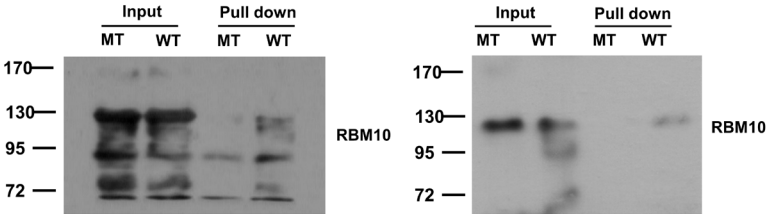

Supplementary Figure 4. Flag-RBM10 was pulldown by biotin-labeled oligos from PCNA-1 cells and detected by western blot using Flag antibody (Original image of **Figure 6D**).